JOURNAL OF SOLID STATE CHEMISTRY **140,** 168–174 (1998)
ARTICLE NO. SC977730

Study of the Solid Solutions of $LiNbO_3$ and $LiTaO_3$ with Mn^{2+}

M. E. Villafuerte-Castrejón

Instituto de Investigaciones en Materiales, Universidad Nacional Autónoma de México, Apdo. Postal 70-360, 04510 México, D. F., Mexico

and

J. A. Azamar-Barrios and P. Bartolo-Pérez

Centro de Investigación y de Estudios Avanzados, Instituto Politécnico Nacional, Apdo. Postal 73 Cordemex, 97310 Mérida, Yucatan, México

Received March 6, 1996; in revised form December 3, 1997; accepted December

Two unusual, extensive new solid solutions of $LiNbO_3$ and $LiTaO_3$ with MnO have been prepared, where $4Mn^{2+}$ replace a combination of $3Li^+$ and a pentavalent cation: Nb^{5+} or Ta^{5+}. The formulas are $Li_{1-x}M_{1-x}Mn_{4x}O_3$, $0<x<0.13$, for $M=Nb$ and $0<x<0.23$ for $M=Ta$. The solid solutions were characterized by X-ray powder diffraction and density measurements. The manganese oxidation states were determined by X-ray photoelectron spectroscopy. © 1998 Academic Press

INTRODUCTION

Doped and undoped $LiNbO_3$ and $LiTaO_3$ have been extensively studied because of their interesting electrical and optical properties. Both unusual materials, which are ferroelectric, have a variety of applications in electrooptics, acoustooptics, and nonlinear optics. $LiNbO_3$ exists on the join Li_2O–Nb_2O_5 as a solid solution series over a composition range of 50 to 56.5% (Nb_2O_5) (1–3), with a congruently melting composition at 51.4% Nb_2O_5. Similarly, $LiTaO_3$ exists over the composition range 49.6 to 54.0% (Ta_2O_5), with a congruently melting composition at 52% Ta_2O_5 (4–6).

Several series of solid solutions of $LiTaO_3$ and $LiNbO_3$ with different cations have been reported (7–18) because of interest in modifying the properties of both compounds by incorporation of impurities into their crystal structures. When Ti^{4+} is introduced into the $LiTaO_3$ lattice, a marked influence on the Curie temperature is observed, which changes from 620–660°C for pure $LiTaO_3$ to 205–500°C for doped compounds, depending on the amount of Ti^{4+} introduced in the lattice. Another application of solid solutions of $LiNbO_3$ and $LiTaO_3$ that contain Eu^{3+} is light-converted materials (19–24). Although some authors have described the optical properties of a single crystal of $LiNbO_3$ with Mn^{2+} (25–34), no one has reported crystallochemical studies of $LiNbO_3$ and $LiTaO_3$ solid solutions with Mn^{2+}. Even though our crystallochemical data were in complete agreement with a divalent valence for manganese when it is incorporated into the lattices of $LiNbO_3$ and the $LiTaO_3$, X-ray photoelectron spectroscopy (XPS) was used to confirm this oxidation state, since this technique has proved to be a very powerful tool for the study of molecular bonding (35, 36).

In this paper we report our experiments related to the crystallochemical study of solid solutions formed by $LiNbO_3$ and $LiTaO_3$ with MnO and our XPS chemical analysis to establish the oxidation state of Mn in the solid solutions.

EXPERIMENTAL

Starting reagents were Li_2CO_3 (reagent grade), Nb_2O_5 (Aldrich, 99.9%), Ta_2O_5 (Aldrich, 99.9%), and MnO (Ventron, 99.5%). Samples, 5 to 10 g total weight, were prepared from appropriate quantities of the starting materials, which were mixed with acetone in an agate mortar and pestle to form a homogeneous paste and dried in Pt crucibles.

Samples were heated at 600–700°C for a few hours to expel CO_2. Additional reheatings were carried out from 1110 to 1200°C for several days with periodic grinding between heating periods. Care was taken to ensure that no significant loss of Li_2O occurred during the firing. To study the purity of the phase, samples were analyzed by X-ray powder diffraction using Cu$K\alpha$ radiation with a Siemens D500. For accurate determination of lattice parameters, a slow scan speed, 0.5° 2θ min^{-1} was used together with KCl as an internal standard. Densities were measured with specific gravity bottles using CCl_4 as the displacement liquid.

The manganese oxidation states were determined by using a Perkin–Elmer (ESCA/SAM) PHI-560 system equipped

0022-4596/98 $25.00

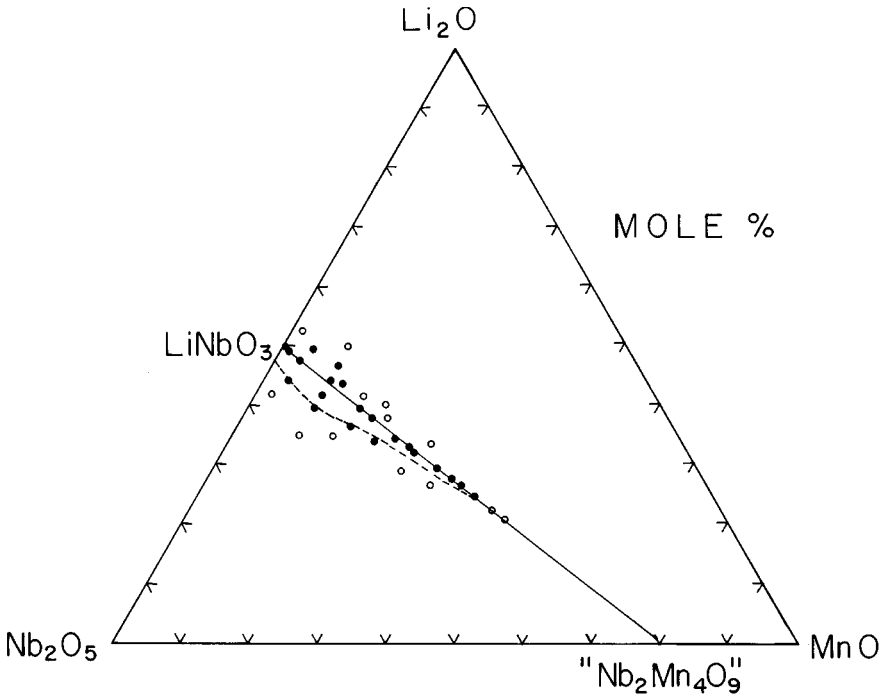

FIG. 1. Solid solution in the system Li_2O–Nb_2O_5–MnO which lie on the stoichiometric join $LiNbO_3$–"$Nb_2Mn_4O_9$". A Li-deficient solid solution area is indicated by the dashed line.

with a double-pass cylindrical mirror analyzer. The samples were bombarded with Mg$K\alpha$ X-rays, which have an energy of about 1.2536 keV. The spectrometer was calibrated with reference to Cu $2p_{3/2}$ (932.4 eV) and $3p_{3/2}$ (74.9 eV). The powder samples and standards were lightly pressed pellets on an indium substrate; these were placed on a stainless-steel holder and introduced into the pretreatment chamber of the spectrometer under a vacuum

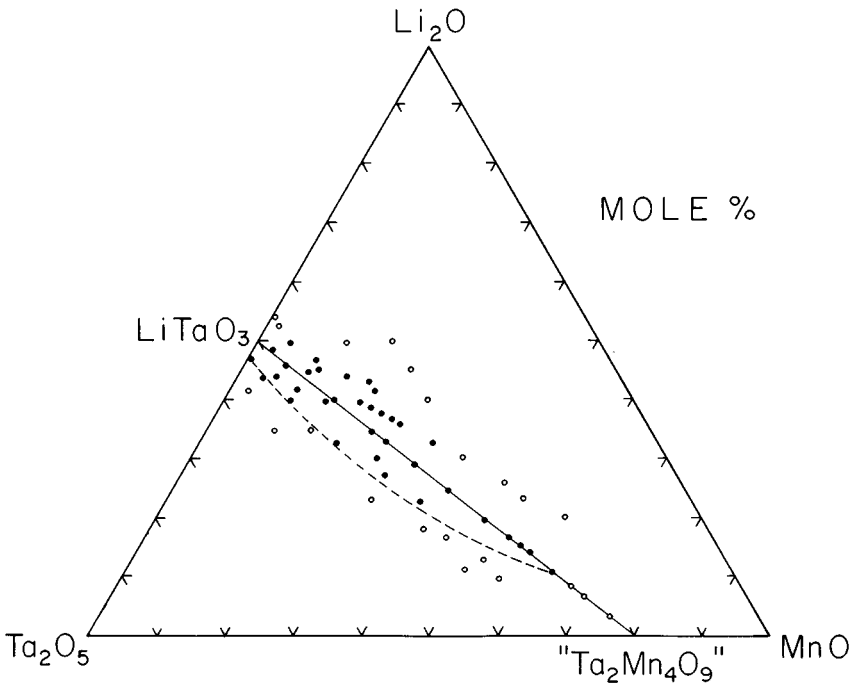

FIG. 2. Solid solution in the system Li_2O–Ta_2O_5–MnO which lie on the stoichiometric join $LiTaO_3$–"$Ta_2Mn_4O_9$". Dashed lines indicate a Li-deficient solid solution area.

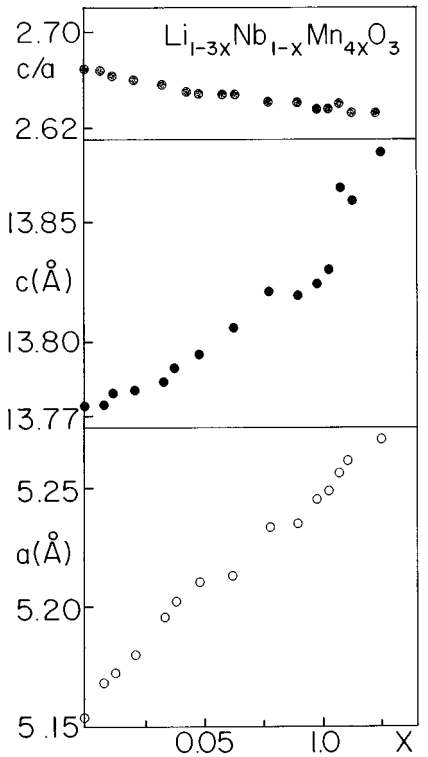

FIG. 3. Variation of the hexagonal lattice parameters a and c of the solid solutions and the ratio c/a as a function of x in the $Li_{1-3x}Nb_{1-x}Mn_{4x}O_3$ solid solution.

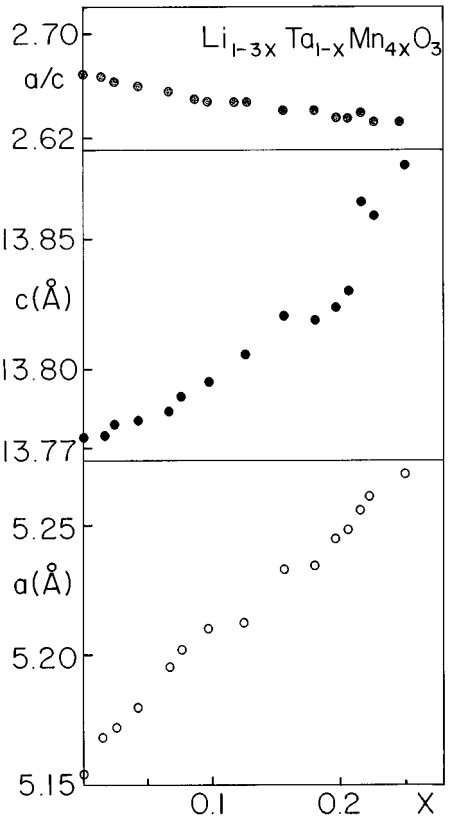

FIG. 4. Variation of the hexagonal lattice parameters a and c of the solid solutions and the ratio c/a as a function of x in $Li_{1-3x}Ta_{1-x}Mn_{4x}O_3$ solid solution

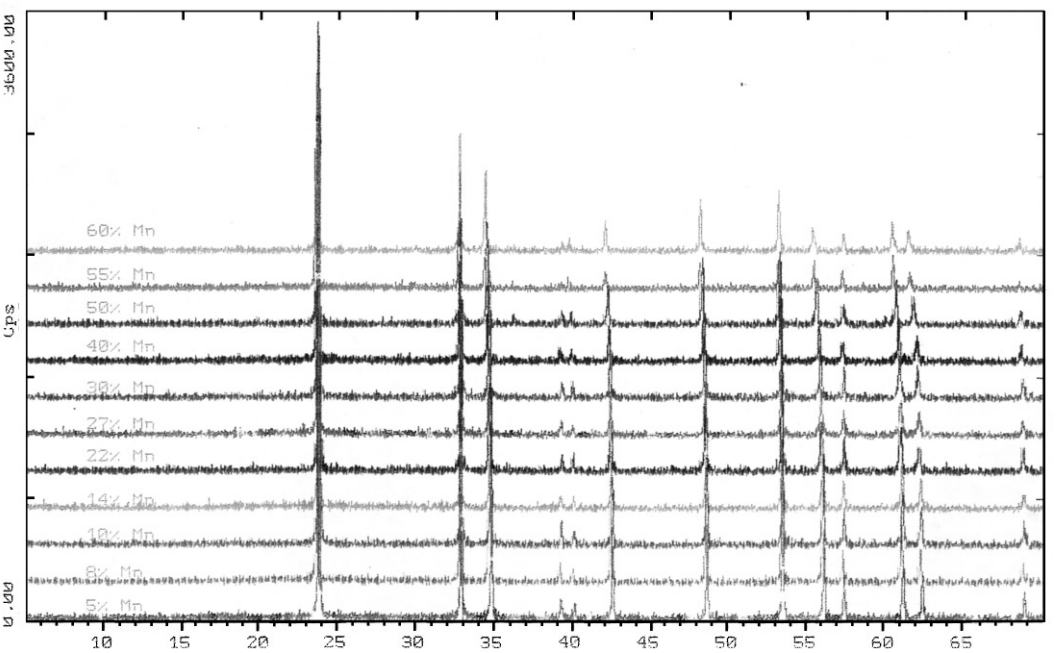

FIG. 5. XRD powder patterns of specimens of the solid solution as a function of mole percentage Mn introduced into the $LiTaO_3$ lattice.

of 1×10^{-7} Torr. A 0.3-cm^2 area of the surface of the samples was sputtered with argon ions. The measurements were carried out at room temperature, in a vacuum of about 2×10^{-9} Torr using a monochromatized X-ray beam with a spot size 3 mm in diameter. The photoelectrons emitted were analyzed with a multichannel position-sensitive detector. The spectral resolution is of the order of 1 eV for the scanning level spectra and 0.2 eV for the valence band spectra. Binding energy was calibrated with reference to *C*1*s* (284.6 eV).

RESULTS AND DISCUSSIONS

Attempts to determine the positions of different cations in $LiNbO_3$ and $LiTaO_3$ have been carried out by a variety of methods to identify the mechanisms of many of their properties. Some effects of divalent cation (Mg, Zn, Ca, Ni) substitution in $LiNbO_3$ single crystals have been reported (6, 37–43). Results of studies in solid solution with Mg in $LiNbO_3$ single crystals with congruent compositions, in the range 45–49 mol% lithium, indicated that Mg ions are incorporated into the Li site. A similar effect of Zn substitution is observed where cation vacancies are produced by the substitution of one Zn^{2+} ion for two Li^+ ions.

The structure of $LiNbO_3$ single crystals has defects caused by lithium deficiency; meanwhile, in stoichiometric powder samples, the structure is close to that of the ideal model, i.e., a sequence of distorted oxygen octahedra joined with their faces along the threefold polar axis *c*. The cations are distributed in the octahedra in the following sequence: Nb, vacancy, Li, Nb, vacancy, Li. For these reasons, results of studies that involve the incorporation of different cations into single crystals and into stoichiometric samples should be different. On the other hand, for $LiTaO_3$ solid solutions with divalent cations (Zn, Ni, Ca, Ni, Ca, Mg), different composition lines in the ternary diagram have been studied in powder samples (18, 44). The upper solubility limit corresponds to the stoichiometric line, except for the $LiTaO_3$–Zn solid solution; in this case the upper solubility limit corresponds to a mechanism in which cation vacancies are created.

Our experimental results show that in each of the ternary systems studied (Li_2O–Nb_2O_5–MnO and Li_2O–Ta_2O_5–MnO), an unusual, wide, wedge-shaped solid solution area can be found (Figs. 1, 2).

Among the reported solid solution series, solid solutions formed with Mn^{2+} have the highest solubility range. Both solid solutions are most extensive in the direction of the hypothetical compounds "$Nb_2Mn_4O_9$" and "$Ta_2Mn_4O_9$", respectively. On the joins $LiNbO_3$–"$Nb_2Mn_4O_9$" and $LiTaO_3$–"$Ta_2Mn_4O_9$" the solid solution mechanisms are such that the total cation content remains constant:

$$3Li^+ + Nb^{5+} \rightarrow 4Mn^{2+} \quad \text{and} \quad 3Li^+ + Ta^{5+} \rightarrow 4Mn^{2+}.$$

This gives the solid solution formulas

$$Li_{1-3x}Nb_{1-x}Mn_{4x}O_3 \quad \text{and} \quad Li_{1-3x}Ta_{1-x}Mn_{4x}O_3.$$

The range of composition, *x*, was found to be of the order of $0 < x < 0.13$ for Nb solid solutions, whereas for Ta solid solutions it was $0 < x < 0.23$. The limiting compositions of $Li_{0.62}Nb_{0.872}Mn_{0.512}O_3$, and $Li_{0.31}Ta_{0.77}Mn_{0.92}O_3$ containing 41 and 63 mol% MnO respectively, were determined. As in all of the solid solutions reported, the solubility range is higher in the $LiTaO_3$ series than in the $LiNbO_3$ solid solutions.

The solid solution areas in the ternary diagrams Li_2O–Nb_2O_5–MnO and Li_2O–Ta_2O_5–MnO are shown in Figs. 1 and 2. From Fig. 1 it is readily observed that the $LiNbO_3$ solid solutions on the join $LiNbO_3$–"$Nb_2Mn_4O_9$" extend to the approximate composition of 24 mol% Li_2O,

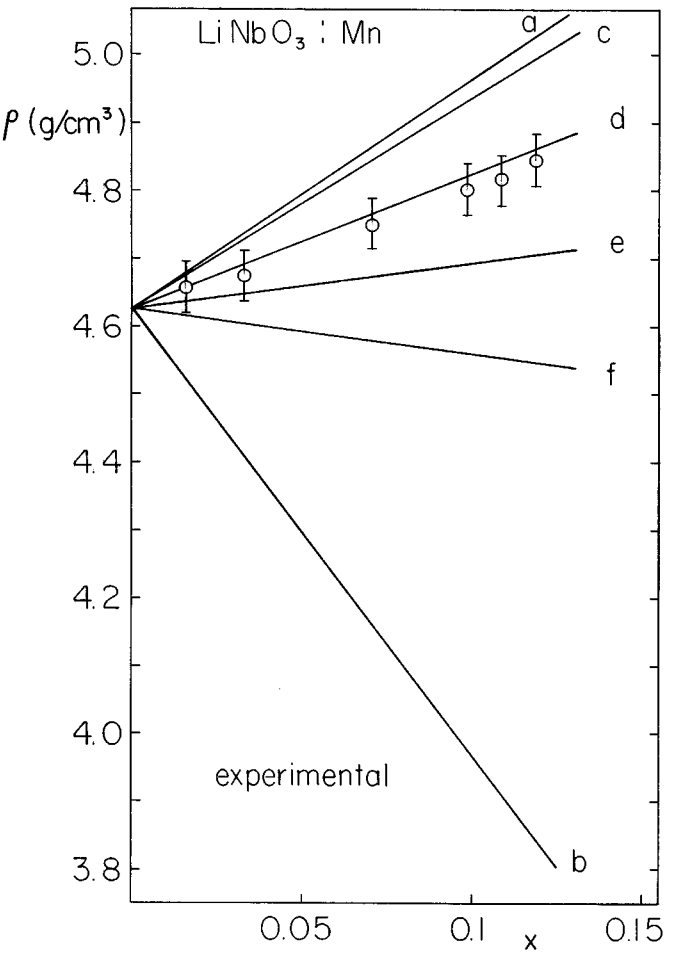

FIG. 6. Experimental and calculated densities of $Li_{1-3x}Nb_{1-x}Mn_{4x}O_3$ solid solutions as a function of *x*, using different Mn replacement mechanisms: (a) $Li^+ + 3M^{5+} \rightarrow 8Mn^{2+}$, (b) $2Li^+ + 4M^{5+} \rightarrow 11\,Mn^{2+}$, (c) $Li^+ + M^{5+} \rightarrow 3\,Mn^{2+}$, (d) $3Li^+ + M^{5+} \rightarrow 4Mn^{2+}$, (e) $5Li^+ + M^{5+} \rightarrow 5\,Mn^{2+}$, (f) $2Li^+ \rightarrow Mn^{2+}$.

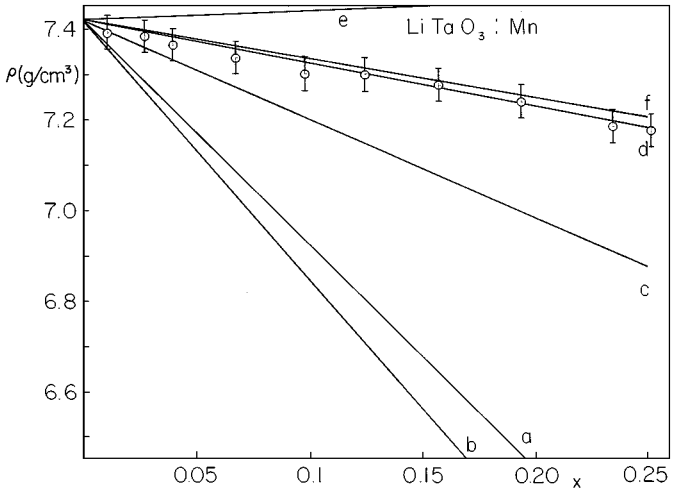

FIG. 7. Experimental and calculated densities of $Li_{1-3x}Ta_{1-x}Mn_{4x}O_3$ solid solutions as a function of x, using different Mn replacement mechanisms as in Fig. 5. 6.

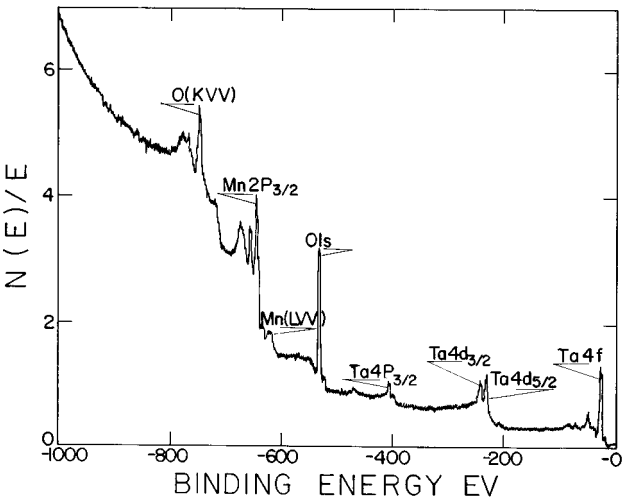

FIG. 9. XPS survey of the $Li_{0.27}Ta_{0.76}Mn_{0.98}O_3$ sample surface.

35 mol% Nb_2O_5, and 41 mol% MnO. From Fig. 2 it seems that the approximate composition limit of the solid solutions on the join $LiTaO_3$–"$Ta_2Mn_4O_9$" is 11 mol% Li_2O, 27 mol% Ta_2O_5, and 62 mol% MnO.

The lattice parameters of one selection of $LiNbO_3$ and $LiTaO_3$ solid solution compositions were determined and the results are shown in Figs. 3 and 4. In both solid solutions the hexagonal a and c parameters show a gradual increase with increasing MnO content, according to Vegard's law. The decrease in the ratio c/a indicates that the expansion of the unit cell in the Nb and Ta systems is anisotropic. In both systems the expansion of c is smaller than that of a and, consequently, the value of the ratio c/a decreases with x. Figure 5 shows the XRD patterns of selected specimens of the solid solution. Intensities of some peaks (006, 113, 202, 024, 116) are considerably affected because of a large difference in atomic scattering factor between Li and Mn.

Experimental and calculated densities are shown in Figs. 6 and 7. The hypothetic lines in the ternary diagram (Fig. 8) represent different substitution mechanisms for solid solution formation. Line (d) corresponds to the proposed substitution mechanism described before as the stoichiometric one: $3Li^+ + M^{5+}$ $(M = Nb, Ta) \rightarrow 4Mn^{2+}$. The experimental data are well consistent with the calculated theoretical values for the proposed stoichiometric substitution. The experimental results are 1 to 3% lower than the calculated

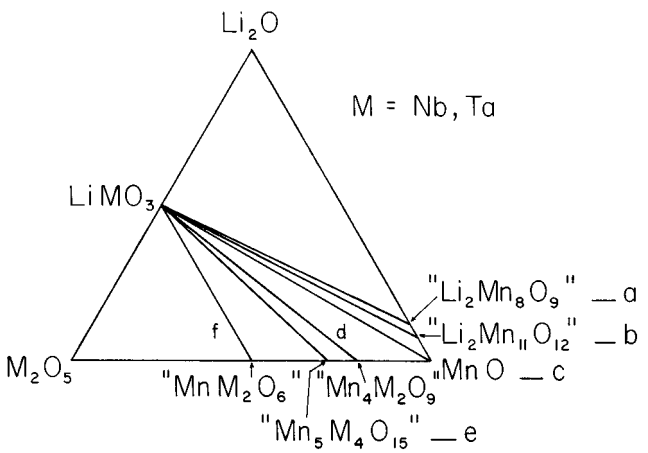

FIG. 8. Hypothetical lines representing different possible solid solutions formed in the systems Li_2O–M_2O_5–MnO (M = Nb, Ta), each corresponding to the mechanisms described in Fig. 5, 6.

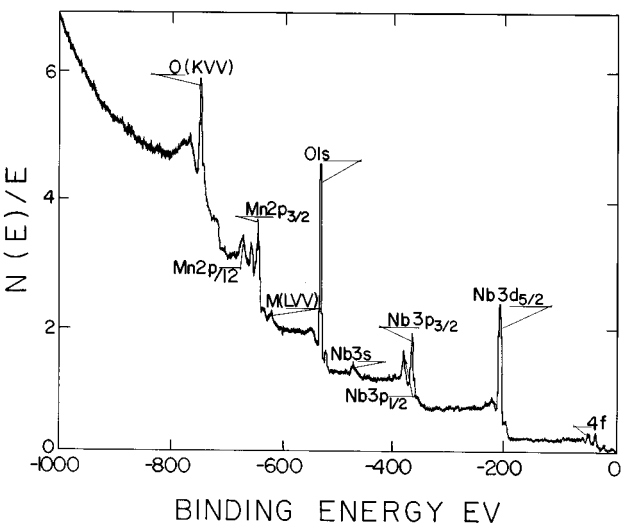

FIG. 10. XPS survey of the $Li_{0.5}Nb_{0.83}Mn_{0.66}O_3$ sample surface.

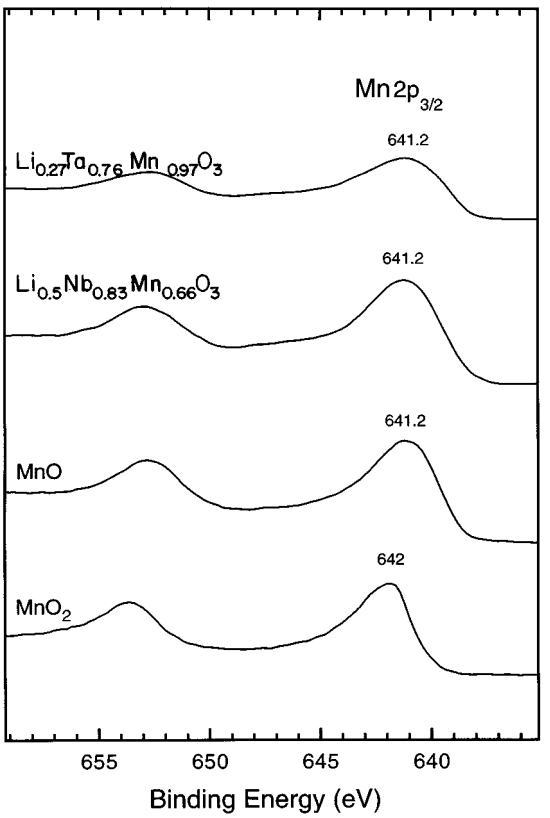

FIG. 11. Manganese $2p_{3/2}$ binding energy: (a) $Li_{0.27}Ta_{0.76}Mn_{0.97}O_3$, (b) $Li_{0.5}Nb_{0.83}Mn_{0.66}O_3$, (c) MnO reference, (d) MnO_2 reference.

theoretical values for this replacement mechanism. This is a common effect of the measurement of densities of powders using liquid displacement and it is attributed to the difficulty in removing residual air on the surface of the particles. The important result, however, is that the experimental data follow quite well the theoretical lines, indicating that the proposed mechanism of solid solution formation is correct. An EPR study of $LiNbO_3$ with Mn^{2+} reports, in accord with our results, that Mn^{2+} ion substitutes for either Li^+ or Nb^{5+} ion in the $LiNbO_3$ lattice (26).

Figures 9 and 10 are low-resolution XPS scans, run on the surface of the two samples. The spectrum displays XPS core-level features of the tantalum and niobium compounds. One more detailed form to manganese $2p_{3/2}$ peaks composed of single component is given in Fig. 11, which shows $Li_{0.27}Ta_{0.76}Mn_{0.97}O_3$, $Li_{0.5}Nb_{0.83}Mn_{0.66}O_3$, MnO, and MnO_2 $2p_{3/2}$ spectral binding energies. The *C*1*s* peak was used as the primary standard binding energy taken to be 284.6 eV; the values are listed in Table 1 (45). From this figure, it is clear that the observed energy of the Mn $2p_{3/2}$ peak (241.2 eV) for the solid solutions coincides with the same energy peak for MnO, showing that the oxidation is broader than the peak of Mn. This fact may be related to the different chemical environments of Mn in these samples.

TABLE 1
Manganese $2p_{3/2}$ Binding Energy, Experimental and Calibrated, with Reference to *C*1*s* (284.6 eV)

	Mn $2p_{3/2}$		*C*1*s*		
	Exp.	Calib.	Exp.	Calib.	ΔeV
$Li_{0.27}Ta_{0.76}Mn_{0.97}O_3$	641.6	641.2	285.0	284.6	0.4
$Li_{0.5}Nb_{0.83}Mn_{0.66}O_3$	642.0	641.2	285.4	284.6	0.8

These results indicated for a comparative study of signal intensities, confirm the identity of the manganese oxidation state, which was found to be Mn^{2+}.

ACKNOWLEDGMENTS

We thank A. Ibarra-Palos, C. Sánchez-Guerrero, and R. Reyes for technical assistance and Dr. J. L. Peña-Chapa for lending us the XPS equipment. We also thank DGAPA, UNAM, for partial support through PAPIIT Program IN105895.

REFERENCES

1. J. R. Carruthers, G. E. Peterson, and M. Grasso, *J. Appl Phys.* **42,** 5 (1975).
2. P. Lerner, C. Legras, and P. Dumas, *J. Cryst. Growth* **3,** 4231 (1968).
3. Räuber, "Chemistry and Physics of Lithium Niobate," Current Topics in Materials Science, Vol. I, North-Holland, Amsterdam, 1978.
4. R. S. Roth, H. S. Parker, W. S. Brower, and J. L. Waring, *in* "Fast Ion Transport in Solids" (W. Van Gool, Ed.), p. 217, North-Holland, Amsterdam, 1973.
5. D. C. Sinclair and A. R. West, *Phys Rev. B* **39,** 13846 (1989).
6. D. A. Brayan, R. Gerson, and H. E. Tomoschke, *Appl. Phys. Lett.* **44,** 847 (1984).
7. C. Kus, M. J. Dambekalne, I. V. Brante, K. J. Bormains, and A. V. Plaude, *Ferroelectrics* **81,** 281 (1988).
8. C. E. Rice, *J. Solid. State. Chem.* **64,** 188 (1986).
9. R. R. Neurgaonkar, T. C. Lim, and L. E. Cross, *Ferroelectrics* **27,** 63 (1980).
10. J. Ravez, G. T. Joo, J. Senegas, and P. Hagenmuller, Proceedings of the Sixth International Meeting on Ferroelectricity, Kobe, 1985, *Jpn. J. Appl. Phys.* **24,** *Suppl.* **24-2,** 1000 (1985).
11. B. Elouadi and M. Zrioui, *J. Solid State Chem.* **64,** 22 (1986).
12. G. T. Joo, J. Senegas, J. Ravez, and P. Hagenmuller, *J. Solid State Chem.* **68,** 247 (1987).
13. M. E. Villafuerte-Castrejón, A. R. West, and J. Rubio O., *Radiat. Effects Defects. Solids* **114,** 175 (1990).
14. F. Agulló-López and J. M. Cabrera, "Properties of $LiNbO_3$" Data Reviews Inspec (1989).
15. G. T. Joo, J. Ravez and P. Hagenmuller, *Rev. Chem. Min.* **22,** 18 (1985).
16. B. Elouadi and F. E. Mouahid, *Phase Transitions* **9,** 221 (1987).
17. K. K. Deb, *J. Mater. Res.* **2**(5), 588 (1987).
18. J. Ravez, R. Von der Mühll, B. Elouadi, and M. Zriouil, *Mater. Res. Bull.* **15,** 483 (1990).
19. L. Arizmendi and J. M. Cabrera, *Phys Rev. B* **31,** 7138 (1984).
20. L. Arizmendi, F. Abella and J. M. Cabrera, *Ferroelectrics* **56,** 75 (1984).

21. H. G. Brittain and W. A. McAllister, *Spectrochim. Acta.* **41,** 1041 (1985).
22. K. S. Bagdasarov, N. Y. Bodanov, E. M. Uyukin, and M. N. Filippdor, *Sov. Phys. Solid State* **29,** 91 (1980).
23. M. E. Villafuerte-Castrejón, A. R. West, and J. Rubio O., *Radiat. Effects Defects Solids* **114,** 175 (1990).
24. M. E. Villafuerte-Castrejón, A. R. West, A. Muñoz F. and J. Rubio O., *Radiat. Effects Defects Solids* **124,** 341 (1992).
25. V. E. Vasil'ev, B. B. Ped'ko, and V. M. Rudyak, *Sov. Phys. Solid State* **29,** 1474 (1987).
26. J. B. Herrington, B. Dischler, and J. Schneider, *Solid State Commun.* **10,** 509 (1972).
27. G. I. Malovichko, V. G. Granchev, and S. N. Lukins, *Sov. Phys. Solid State* **28,** 553 (1986).
28. G. I. Malavichko, A. A. Karmuzin, I. P. Bykov, V. V. Layuta, and V. P. Yarunichev, *Sov. Phys. Solid State* **25,** 2038 (1983).
29. G. I. Malovichko, M. D. Glinchuk, A. A. Karmazin, I. P. Bykov, and V. P. Yarumichev, *Soc. Phys. Solid State* **27,** 97 (1985).
30. V. G. Grachev and G. I. Malovichko, *Sov. Phys. Solid State* **27,** 424 (1985).
31. G. I. Malovichko and V. G. Gracker, *Sov. Phys. Solid State* **27,** 1678 (1985).
32. B. Dischler, J. R. Herrington, A. Räuber, and H. Kurz, *Solid State Commun.* **14,** 1233 (1974).
33. Kh. S. Bagdasarov, B. N. Grechshnikov, V. F. Karyagin, and E. M. Uyukin, *Pis'ma Zh. Tekh. Fiz.* **11,** 420 (1985).
34. D. G. Rexford and Y. M. Kim, *J. Chem. Phys.* **57,** 3094 (1972).
35. S. Laarst, T. Anderson, and J. C. Otamiri, *Appl. Surf. Sci.* **45**, 1 (1990).
36. A. R. González-Elipe, J. P. Espinos, A. Fernández, and G. Manuera, *Appl. Surf. Sci.* **45**, 103 (1990).
37. K. L. Sweeney, L. E. Halliburton, D. A. Bryan, R. R. Rice, R. Gerson, and H. E. Tomaschke, *J. Appl. Phys.* **57**, 4 (1985).
38. R. H. Holmes, Y. S. Kim, C. D. Brandle, and D. M. Smyth, *Ferroelectrics* **51** (1983).
39. S. Kawakami, E. Ishii, A. Tsuzuki, T. Sekiya, and Y. Torii, *Mater. Res. Bull.* **21**, (1986).
40. N. Iyi, K. Kitamura, Y. Yajima, S. Kimura, Y. Furukawa, and M. Sato, *J. Solid State Chem.* **118**, 148 (1995).
41. B. C. Grabmaier and F. Otto, *J. Cryst. Growth* **79**, (1986).
42. H. J. Donnerberg, S. M. Tomlinson, and C. R. A. Catlow, *J. Phys. Chem. Solids* **52**, 1 (1992).
43. B. C. Grabmaier, W. Wersing, and W. Koestler, *J. Cryst. Growth* **110**, (1991).
44. Y. Torii, T. Sekiya, T. Sekiya, T. Yamamoto, K. Koyabashi, and Y. Abe *Mater. Res. Bull.* **18,** 12 (1983).
45. C. D. Wagner, W. M. Riggs, L. E. Davis, J. F. Moulder, and G. E. Muilenberg (Eds.), "Handbook of X-ray Photoelectron Spectroscopy," Perkin-Elmer, Physical Electronics, Eden Prairie, MN, 1979.